International Journal of Fluid Power 10 (2009) No. 3 pp. 5-16

ACTIVE VIBRATION DAMPING FOR AN OFF-ROAD VEHICLE WITH DISPLACEMENT CONTROLLED ACTUATORS

Christopher Williamson[1], Shinok Lee[2], and Monika Ivantysynova[1,2]

[1]*Purdue University, Department of Agricultural and Biological Engineering, 225 S. University St., West Lafayette, Indiana 47907, USA*
[2]*Purdue University, School of Mechanical Engineering, 225 S. University St., West Lafayette, Indiana 47907, USA*
williaca@purdue.edu, lee20@purdue.edu, mivantys@purdue.edu

Abstract

Mobile earthmoving machines typically do not have wheel suspension. Consequently, vehicle dynamics are underdamped, and operators experience vibrations of low frequency and high amplitude which are detrimental to health, comfort and productivity. For most vehicles, the state of the art for improving ride quality is passive energy dissipation via seat dampers and hydraulic accumulators connected in parallel to the actuators. Alternatively, ride quality may be enhanced by active control of the seat or working actuators. In the present work, active vibration damping is considered for a skid-steer loader based on control of the flow rate to the boom lift cylinders with a variable displacement pump. A four degrees of freedom vehicle dynamic model is derived for linear motion in the vertical and horizontal directions, pitching angle, and boom motion with respect to the chassis. Dynamics of the hydraulic pump and actuator are also modelled. Considering the requirements of the intended application, the feedback control design emphasizes simplicity of implementation. The control law is a multi-DOF version of the well-known "skyhook damper" principle, where the control force is proportional to the vehicle velocity. Cascaded feedback loops of pump displacement and pressure produce the required force. An experimental evaluation was conducted according to ISO 2631-1 (1997) to measure the effect of the active controller on whole-body vibration as perceived by the operator. The active damping system reduced total vibration by as much as 34% and was consistently superior to a commercially available passive damping solution. Another controller with only pressure and position feedback was also tested; its performance was similar to the passive accumulators.

Keywords: active vibration damping, active suspension, displacement control, pump control, pressure control, loader

1 Introduction

Many off-road vehicles such as wheel loaders, skid-steer loaders, tractors and backhoes have no wheel suspension. Although necessary for stiffness while carrying loads, the lack of suspension causes poor ride characteristics, including low frequency vehicle oscillations. Low frequency vibration is detrimental to the comfort and safety of the operator (ISO 2631-1, 1997) and may limit the maximum travel speed of the vehicle.

1.1 State of the Art

The most common solution for reducing vibration in mobile loaders involves adding passive devices to increase the damping of the hydraulic system. One or more accumulators are connected in parallel to the boom lift cylinders. The accumulators dissipate kinetic energy through flow restriction losses as the boom oscillates relative to the vehicle chassis. Passive "ride control" systems are commercially available for many wheel loaders and skid-steer loaders. This technique considerably improves the ride characteristics. Latour and Biener (2002) demonstrated >40% amplitude reduction in pressure oscillations on a small wheel loader with accumulators for vibration damping. One disadvantage of this approach is that the accumulators reduce the actuator stiffness necessary for lifting and moving loads. Consequently, additional components must be added to disconnect the accumulators while the cylinders are working and to equalize the actuator and accumulator pressures before reconnecting.

An alternative strategy is active vibration damping, in which an electronic controller, sensors, and electrohydraulic valves are used to reduce oscillation. Compared to traditional passive damping techniques, active damping

This manuscript was received on 30 March 2008 and was accepted after revision for publication on 25 August 2009

offers greater performance and flexibility. Researchers have investigated active damping for wheel loaders, agricultural tractors, excavators, and other mobile applications. Most of these projects used the existing actuator control valves for vibration damping. A few strategies involving an additional control valve have also been proposed. The review paper by Rahmfeld and Ivantysynova (2004) provides a good summary of this research.

The majority of the previous research for wheel loaders and tractors has focused on reducing vibration by controlling actuator pressure and position. A few publications have considered acceleration feedback (Berger and Patel, 1999; Frediani et al., 2004; Rahmfeld and Ivantysynova, 2003) in the vertical direction only. A single paper in the literature considers active damping for a skid-steer loader (Hansen, Andersen and Conrad, 2002). A novel strategy for reducing pitch oscillation by controlling the drive motor torque was proposed, but no measurements were published. In nearly all of the existing literature, the control systems for active damping are based on classical single-input, single-output feedback loops for position, pressure, etc. which are summed to form the command signal.

Operator comfort may also be improved by active or semi-active damping of the operator's seat. Active control of seat vibration is commercially available on some large agricultural tractors and also has been the subject of academic research by multiple authors. The interested reader is referred to (Klooster, 2004) for a comprehensive bibliography.

One weakness of previous research is the lack of rigorous experimental evaluation. From the papers cited here, it is unclear to what extent reductions in the measured variables (e.g. hydraulic pressure, machine acceleration) correspond to improvements in quantities of interest such as operator comfort and machine productivity. The present work attempts to fill this gap by adherence to international measurement standards (ISO 2631-1, 1997).

1.2 Active Damping with Displacement Control

Displacement-controlled (DC) actuation refers to a variable displacement pump connected to a single or double-rod cylinder in a closed hydraulic circuit, as in Fig. 1. This "valveless" or "pump-controlled" concept offers several advantages over traditional valve control, including higher efficiency and linear dynamic characteristics. Other DC circuit configurations exist, such as the open-circuit solution developed by Heybroek (2008). Active vibration damping using DC actuators was first proposed by Rahmfeld and Ivantysynova (2003) with application to a medium-sized wheel loader. Measurements of vertical cabin acceleration and cylinder pressure showed amplitude reductions up to 30% with active control (Rahmfeld, Ivantysynova and Eggers, 2004). In simulations comparing active damping using load-sensing valve control and pump displacement control for this application, the DC solution required 45-60% less energy for position and acceleration control, depending on the bucket load (Eggers, Rahmfeld and Ivantysynova, 2005).

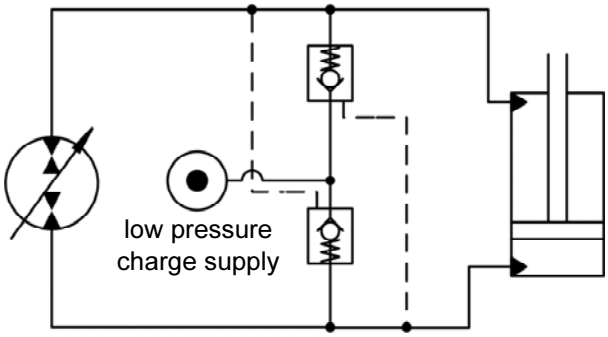

Fig. 1: *Basic displacement control circuit*

1.3 DC Skid-steer Loader

More recently, the authors have developed a similar DC hydraulic system for a 3.5 ton skid-steer loader (Fig. 2). Although the primary objective of the project was to conserve fuel, an active control system for improving operator comfort adds value for the additional cost of only a few sensors. The goal of the present work is then to design and test a method for reducing vehicle vibration with DC actuators. The original contribution of this paper compared to previous publications is a more sophisticated dynamic model and control law, along with better experimentation.

The authors present a dynamic model of the loader hydraulic system and a 4-DOF model of vehicle motion in section 2. Control design and analysis are covered in section 3. Section 4 reports measurements for parameter identification and model validation as well as an experimental evaluation of the control system.

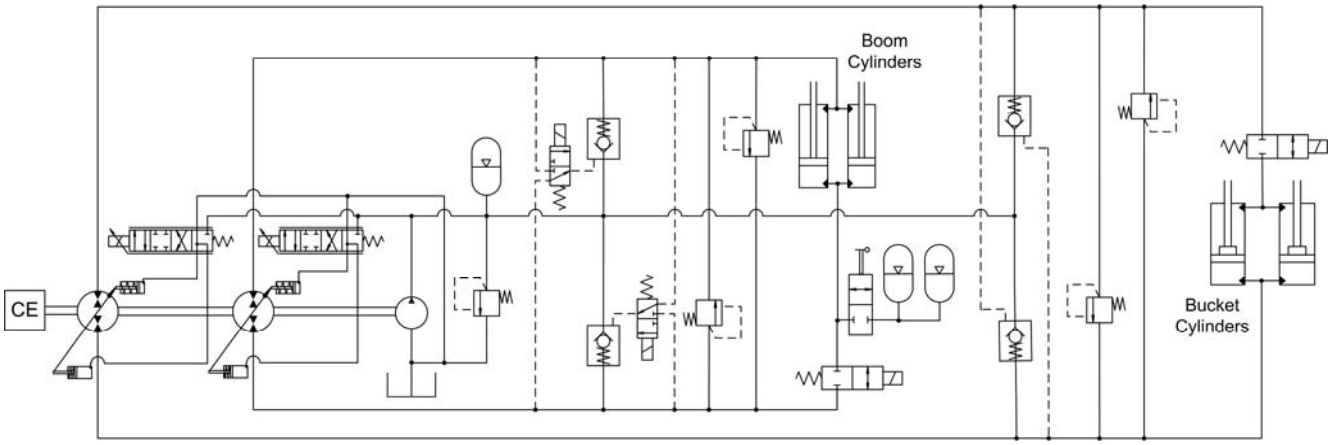

Fig. 2: *Hydraulic schematic of DC skid-steer loader boom and bucket functions*

2 Mathematical Model

This section covers the derivation of an analytical model of the machine dynamics. A more detailed, numerical simulation model was also constructed in Matlab/Simulink (Williamson and Ivantysnova, 2007).

2.1 Multi-body Vehicle Dynamics

The multi-body dynamics of the skid-steer loader are modeled with the Newton-Euler method, in which equations of motion are written for each body individually and then combined by the forces and kinematic constraints between them. Planar motion and rigid bodies are assumed.

A side view of the skid-steer loader is shown in Fig. 3. The wheel axles and boom joints are labeled alphabetically. The global coordinate origin is defined at point O, the location of the loader's center of gravity at equilibrium. The origin is fixed in space and does not translate or rotate as the machine moves. All forces, torques and accelerations are calculated with respect to these Cartesian coordinates. A local coordinate frame is attached to each body at its center of gravity and is used to define position vectors and body orientation.

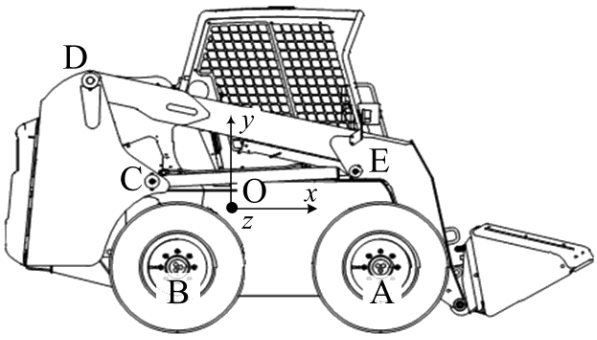

Fig. 3: *Loader geometry, reference points and global coordinate frame*

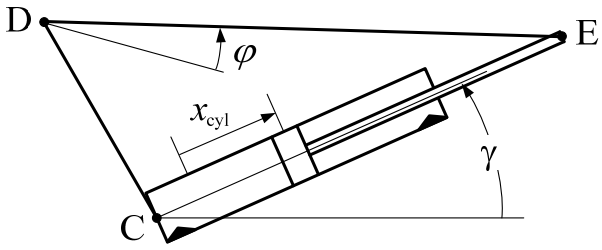

Fig. 4: *Definition of actuator geometry*

Since the loader has no mechanical suspension, ride characteristics are dominated by the tires. The tires are modeled as simple spring-dampers in two orthogonal directions, as in Fig. 5 and Eq. 1 to 4. Planar motion is assumed, so only two tires are modelled (i.e. the left and right sides are lumped together). The loader weight F_{g1} is eliminated from the equations of motion by measuring the axle positions from static equilibrium.

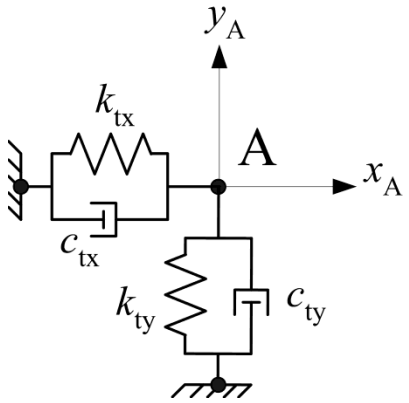

Fig. 5: *2-DOF linear tire model*

$$F_{Ay} = -k_{ty} y_A - c_{ty} \dot{y}_A \tag{1}$$

$$F_{Ax} = -k_{tx} x_A - c_{tx} \dot{x}_A \tag{2}$$

$$F_{Bx} = -k_{tx} x_B - c_{tx} \dot{x}_B \tag{3}$$

$$F_{By} = -k_{ty} y_B - c_{ty} \dot{y}_B \tag{4}$$

Body 1 is the frame or chassis of the loader, illustrated in Fig. 6. Position and orientation are measured at point H from the global coordinate frame at point O. Point H is the center of mass of the loader chassis and coincides with point O when the machine is at rest. The chassis orientation θ_1 is the angle of rotation about the z-axis.

Summing forces and moments about H, the equations of motion for the chassis are given in Eq. 5 to 7. F_{dx}, F_{dy} and M_d are disturbance forces and moments due to driving over uneven terrain. For notational simplicity, these disturbances are modelled as being applied directly to the chassis center of gravity rather than at the tire surfaces. Vehicle motion in the vertical direction y is termed bounce or heave, and angular motion in the θ direction is called pitch.

$$F_{Ax} + F_{Bx} + F_{Cx} + F_{D12x} + F_{dx} = m_1 \ddot{x}_H \tag{5}$$

$$F_{Ay} + F_{By} + F_{Cy} + F_{D12y} + F_{dy} = m_1 \ddot{y}_H \tag{6}$$

$$\begin{aligned} &F_{Ax} r_{AHy} + F_{Ay} r_{AHx} + F_{Bx} r_{BHy} - F_{By} r_{BHx} + M_d \\ &- F_{Cx} r_{CHy} - F_{Cy} r_{CHx} - F_{D12x} r_{DHy} - F_{D12y} r_{DHx} \\ &= J_1 \ddot{\theta}_1 \end{aligned} \tag{7}$$

Distances between points on a body are defined as in Eq. 8 to 9, where θ_{AH} is the constant angle and r_{AH} is the constant distance between points A and H on body 1. Forces are defined by their direction and point of application. For example, F_{Ax} is the force at A in the global x-axis direction.

$$r_{AHx} = \mathrm{abs}\left(r_{AH} \cos\left(\theta_1 + \theta_{AH}\right)\right) \tag{8}$$

$$r_{AHy} = \mathrm{abs}\left(r_{AH} \sin\left(\theta_1 + \theta_{AH}\right)\right) \tag{9}$$

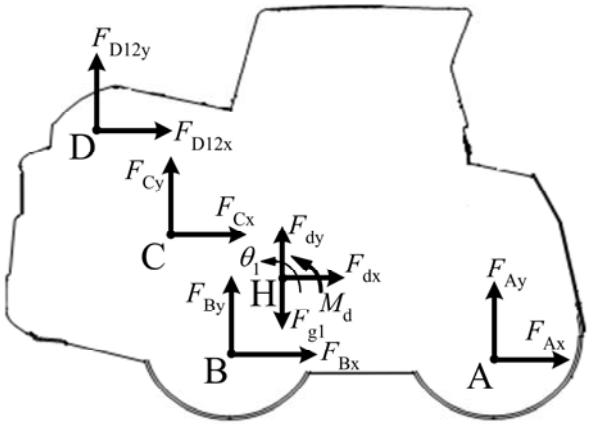

Fig. 6: *Chassis force diagram*

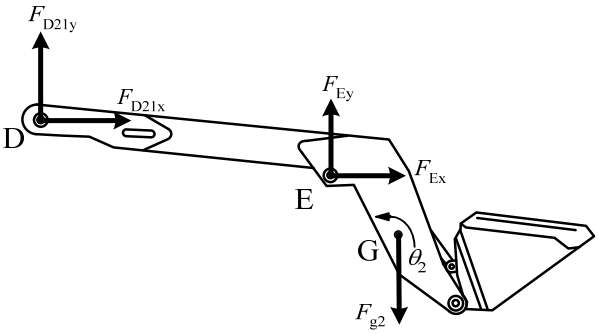

Fig. 7: *Boom force diagram*

Fig. 7 depicts the forces on the loader boom. For modeling purposes, the bucket is assumed to remain in a fixed position relative to the boom. The center of mass of the boom and bucket together is located at G. Summing forces and moments for the boom gives Eq. 10 to 12. As before, the gravitational force drops out of the equations by defining positions and the actuator force to be zero at static equilibrium.

$$F_{D21x} + F_{Ex} = m_2 \ddot{x}_G \tag{10}$$

$$F_{D21y} + F_{Ey} = m_2 \ddot{y}_G \tag{11}$$

$$\begin{aligned} &-F_{D21x} r_{DGy} - F_{D21y} r_{DGx} - F_{Ex} r_{EGy} - F_{Ey} r_{EGx} \\ &= J_2 \ddot{\theta}_2 \end{aligned} \tag{12}$$

Internal forces between the boom and chassis at D are equal and opposite, as in Eq. 13 to 14.

$$F_{D21x} = -F_{D12x} \tag{13}$$

$$F_{D21y} = -F_{D12y} \tag{14}$$

The forces at C and E are a function of the hydraulic actuator force F_{act}, defined later in Eq. 31.

$$F_{act} \cos\gamma = F_{Ex} = -F_{Cx} \tag{15}$$

$$F_{act} \sin\gamma = F_{Ey} = -F_{Cy} \tag{16}$$

Since the boom rotates about the chassis and remains connected at point D, kinematic constraints must be added to the equations of motion. A closed loop of position vectors is constructed from the global origin O to the axis of rotation D through both bodies (Eq. 17). The second derivative of Eq. 17 gives the constraint equations for the body accelerations (Eq. 18 and 19).

$$\boldsymbol{r}_{HO} + \boldsymbol{r}_{DH} = \boldsymbol{r}_{GO} + \boldsymbol{r}_{DG} \tag{17}$$

$$\begin{aligned} \ddot{x}_G &= -r_{DH} \cos(\theta_{DH} + \theta_1) \dot{\theta}_1^2 \\ &- r_{DH} \sin(\theta_{DH} + \theta_1) \ddot{\theta}_1 + r_{DG} \cos(\theta_{DG} + \theta_2) \dot{\theta}_2^2 \\ &+ r_{DG} \sin(\theta_{DG} + \theta_2) \ddot{\theta}_2 + \ddot{x}_H \end{aligned} \tag{18}$$

$$\begin{aligned} \ddot{y}_G &= -r_{DH} \sin(\theta_{DH} + \theta_1) \dot{\theta}_1^2 \\ &+ r_{DH} \cos(\theta_{DH} + \theta_1) \ddot{\theta}_1 + r_{DG} \sin(\theta_{DG} + \theta_2) \dot{\theta}_2^2 \\ &- r_{DG} \cos(\theta_{DG} + \theta_2) \ddot{\theta}_2 + \ddot{y}_H \end{aligned} \tag{19}$$

Combining Eq. 10 to 14 with Eq. 5 to 7 yields the remaining equations of motion for the skid-steer loader.

$$m_1 \ddot{x}_H + m_2 \ddot{x}_G - F_{Ax} - F_{Bx} - F_{dx} = 0 \tag{20}$$

$$m_1 \ddot{y}_H + m_2 \ddot{y}_G - F_{Ay} - F_{By} - F_{dy} = 0 \tag{21}$$

$$\begin{aligned} &-r_{DHy} m_2 \ddot{x}_G - r_{DHx} m_2 \ddot{y}_G + J_1 \ddot{\theta}_1 - F_{Ax} r_{AHy} \\ &- F_{Ay} r_{AHx} - F_{Bx} r_{BHy} + F_{By} r_{BHx} - M_d \\ &= F_{Ex} (r_{CHy} - r_{DHy}) + F_{Ey} (r_{CHx} - r_{DHx}) \end{aligned} \tag{22}$$

$$\begin{aligned} &r_{DGy} m_2 \ddot{x}_G - r_{DGx} m_2 \ddot{y}_G + J_2 \ddot{\theta}_2 \\ &= F_{Ex} (r_{DGy} - r_{EGy}) + F_{Ey} (r_{DGx} - r_{EGx}) \end{aligned} \tag{23}$$

Define a generalized coordinate vector $\boldsymbol{q}$ and Eq. 20 to 23 can be written compactly as a matrix equation (Eq. 25).

$$\boldsymbol{q} = \begin{pmatrix} x_G & y_G & x_H & y_H & \theta_1 & \theta_2 \end{pmatrix}^T \tag{24}$$

$$\begin{aligned} &\mathbf{M}(\boldsymbol{q}) \ddot{\boldsymbol{q}} + \boldsymbol{C}(\boldsymbol{q}, \dot{\boldsymbol{q}}) + \boldsymbol{K}(\boldsymbol{q}) + \boldsymbol{D}(\dot{\boldsymbol{q}}) \\ &= \boldsymbol{F}_{act}(\boldsymbol{q}, \dot{\boldsymbol{q}}, p_A, p_B) \end{aligned} \tag{25}$$

M contains masses and inertias, ***C*** represents centrifugal forces, ***K*** is a vector of forces due to tire stiffness, ***D*** is a vector of tire damping forces and $\boldsymbol{F}_{act}$ is a vector of actuator forces and torques. Actuator and joint friction is lumped with the actuator force vector.

2.2 Modal Analysis

Before proceeding to the hydraulic system model, a vibration analysis will give more insight into the dynamics of the vehicle model derived in the previous section. To study undamped free vibrations, the coefficient matrices from Eq. 25 are linearized with the assumption that the coordinates ***q*** remain within a small region about a single operating point. Damping and centripetal terms are neglected, which are small anyway. Equations 18 and 19 are substituted into Eq. 20 to 23 so that the new coordinate vector ***p*** contains only the independent degrees of freedom. The equations of motion can then be written as Eq. 27. The coefficient matrices are expanded in Eq. 32 to 34.

$$\boldsymbol{p} = \begin{pmatrix} x_H & y_H & \theta_1 & \theta_2 \end{pmatrix}^T \tag{26}$$

$$\mathbf{M}\ddot{\boldsymbol{p}} + \mathbf{K}\boldsymbol{p} = 0 \tag{27}$$

$$k_{eq} = A_p^2 K_{oil} \left(\frac{1}{V_A} + \frac{1}{V_B} \right) \tag{28}$$

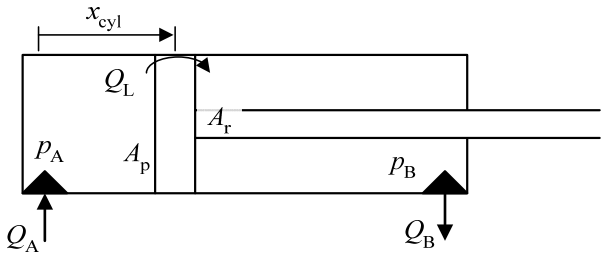

Fig. 8: *Single rod actuator*

For this analysis, the hydraulic actuator is assumed to behave like a linear spring whose equivalent stiffness is due to the fluid compressibility, as in Eq. 28. The undamped natural frequencies and mode shapes of the system can be found by solving Eq. 27. The eigenvalues of $-\mathbf{M}^{-1}\mathbf{K}$ are listed across the top row of Table 1 with the normalized eigenvectors below. As evidenced by Table 1, the vibration modes are strongly coupled.

$$\mathrm{eig}\left(-\mathbf{M}^{-1}\mathbf{K}\right)=\begin{pmatrix}\omega_1^{\,2} & 0 & 0 & 0\\ 0 & \omega_2^{\,2} & 0 & 0\\ 0 & 0 & \omega_3^{\,2} & 0\\ 0 & 0 & 0 & \omega_4^{\,2}\end{pmatrix} \tag{29}$$

Table 1: Natural frequencies and mode shapes

Mode	ω_1	ω_2	ω_3	ω_4
Freq. (Hz)	13.4	5.6	4.8	2.9
x_H	0.22	1.00	0.43	-0.78
y_H	0.22	-0.65	0.89	-0.10
θ_1	1.00	-0.08	-0.39	0.39
θ_2	-0.70	0.37	1.00	1.00

2.3 Hydraulic Actuator Dynamics

The loader's lift cylinders are single-rod, double-acting linear actuators, as shown in Fig. 8. The piston area ratio α is defined as the ratio of the annular area on the rod side to the total surface area of the piston.

$$\alpha=\frac{A_p-A_r}{A_p} \tag{30}$$

The net actuator force is defined in Eq. 31, where F_f represents force due to friction (see section 4.1.1). As noted previously, p_A and p_B are defined to be zero at steady state.

$$F_{act}=A_p\left(p_A-\alpha p_B\right)-F_f \tag{31}$$

Referring to Fig. 4, φ is the boom angle relative to the chassis, which is defined as $\varphi=\theta_2-\theta_1$. The actuator's linear velocity can be related to the angular velocity of the boom with its kinematic Jacobian, as in Eq. 35.

$$\mathbf{M}=\begin{pmatrix} m_1+m_2 & 0 & -r_{DHy}m_2 & r_{DGy}m_2\\ 0 & m_1+m_2 & -r_{DHx}m_2 & r_{DGx}m_2\\ -r_{DHy}m_2 & -r_{DHx}m_2 & (r_{DHy}^2+r_{DHx}^2)m_2+J_1 & -(r_{DHy}r_{DGy}+r_{DHx}r_{DGx})m_2\\ r_{DGy}m_2 & r_{DGx}m_2 & -(r_{DHy}r_{DGy}+r_{DHx}r_{DGx})m_2 & (r_{DGy}^2+r_{DGx}^2)m_2+J_2\end{pmatrix} \tag{32}$$

$$\mathbf{K}=\begin{pmatrix} -2k_{tx} & 0 & -(r_{AHy}+r_{BHy})k_{tx} & 0\\ 0 & -2k_{ty} & -(r_{AHx}-r_{BHx})k_{ty} & 0\\ -(r_{AHy}+r_{BHy})k_{tx} & -(r_{AHx}-r_{BHx})k_{ty} & K_{33} & -\dfrac{\partial x}{\partial\varphi}(r_{CHy}-r_{DHy})k_{eq}\\ 0 & 0 & -\dfrac{\partial x}{\partial\varphi}(r_{CHy}-r_{DHy})k_{eq} & \dfrac{\partial x}{\partial\varphi}(r_{CHy}-r_{DHy})k_{eq}\end{pmatrix} \tag{33}$$

$$K_{33}=-\left(r_{AHy}^2+r_{BHy}^2\right)k_{tx}-\left(r_{AHx}^2+r_{BHx}^2\right)k_{ty}+\frac{\partial x}{\partial\varphi}\left(r_{CHy}-r_{DHy}\right)k_{eq} \tag{34}$$

$$\dot{x}_{\text{cyl}} = \frac{\partial x_{\text{cyl}}}{\partial \varphi}\dot{\varphi} \tag{35}$$

Pressure in the cylinder chambers is a function of flow rate and piston velocity. Internal leakage Q_{L} across the piston seals is defined in section 4.1.2 and external leakage is neglected.

$$\dot{p}_{\text{A}} = \frac{K_{\text{oil}}}{V_{\text{A}}}\left[Q_{\text{A}} - A_{\text{p}}\dot{x}_{\text{cyl}} - Q_{\text{L}}\right] \tag{36}$$

$$\dot{p}_{\text{B}} = \frac{K_{\text{oil}}}{V_{\text{B}}}\left[-Q_{\text{B}} + \alpha A_{\text{p}}\dot{x}_{\text{cyl}} + Q_{\text{L}}\right] \tag{37}$$

2.4 Pump Dynamics

The heart of the DC hydraulic system is a variable displacement pump. On the DC skid-steer loader, the boom cylinders are connected to a 46 cc/rev, axial piston swash plate controlled with a high-speed proportional valve (40 l/min at 75 bar, 90 Hz -3 dB bandwidth at ± 10 %) and an angular sensor for swash plate position feedback.

Pump dynamic modelling and control design were considered in detail by Grabbel and Ivantysynova (2005). The authors of the current work created a similar pump model and designed a gain-scheduled proportional control law for displacement feedback. For purposes of modelling and simulation, the closed-loop pump dynamics can be closely approximated by a rate-limited second order transfer function, as in Fig. 9. $V_{\text{p,ref}}$ is the desired pump displacement and V_{p} is the actual pump displacement. Parameter values are listed in Table 2. The low-amplitude bandwidth of the pump is primarily determined by the dynamic characteristics of the control valve (Grabbel and Ivantysynova, 2005). For larger displacements, the swash plate speed is limited by the flow rate through the control valve. Since the control pressure is rather low (20 bar), this flow saturation effect is significant.

Table 2: Pump dynamic parameters

Parameter	Value	Unit
ω_{p}	22.3	Hz
ζ_{p}	0.53	-
$\dot{V}_{\text{p,max}}$	±1.24	m^3/s

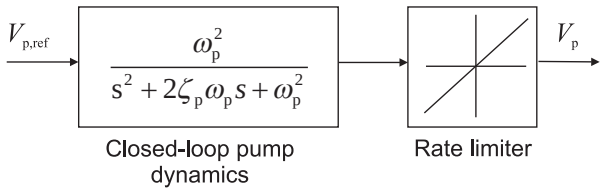

Fig. 9: *Simplified model of pump and control valve dynamics with displacement feedback*

2.5 Model Validation

Simulation results were compared to measured data to check the accuracy of the previously developed model. Fig. 10 shows the free response of the skid-steer loader while driving over a single obstacle at 17 km/h, transformed to the frequency domain The plots clearly show peaks at roughly 2 and 4 Hz, close to the expected mode frequencies from Table 1. The other two modes have lower amplitudes and are not as prominent in the data.

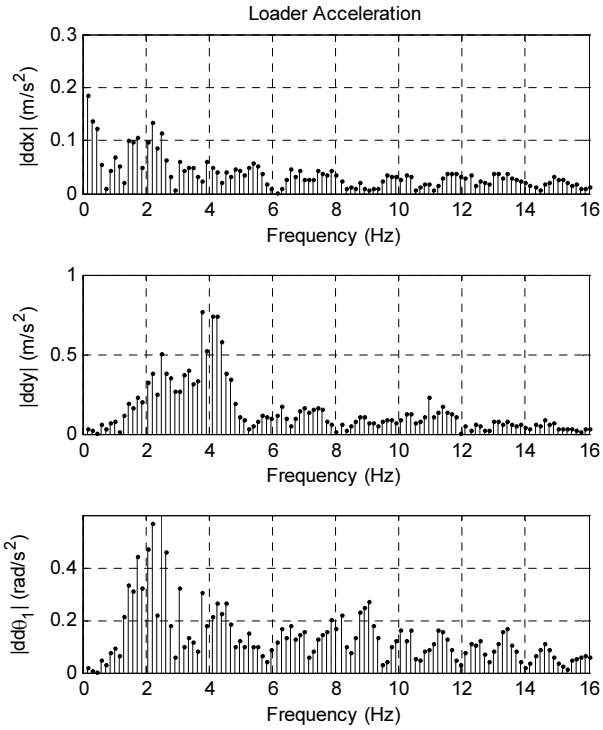

Fig. 10: *Frequency spectra of measured chassis acceleration in the x, y and θ directions*

3 Control System

3.1 Preliminary Considerations

Low frequency vibrations while driving are induced by disturbance forces on the wheels from rough terrain. For active damping, the control problem is to vary the flow rate to the boom lift actuator such that the vibration caused by output disturbances is reduced. The skid-steer loader application requires that the control system be relatively simple, requiring no additional actuators, inexpensive sensors and low computational requirements. For this reason, the authors opted for simplicity where possible in the control design.

Active vehicle suspension systems are often designed by optimal control techniques, where the objective function represents a tradeoff between measures of performance and comfort (Hrovat, 1997). LQR and H_2/H_∞ techniques lead directly to a linear control law based on state feedback. Such an approach was attempted previously for the DC skid-steer loader (Williamson, 2007). There are several important disadvantages to such a design. Most of the system states (namely chassis position and velocity in several directions) cannot be readily measured. These states are observable and can be estimated based on measurable outputs, but an observer requires more computational effort and is sensitive to variations in model parameters. Moreover, such a design does not explicitly con-

sider the undesirable interaction between plant and actuator dynamics (Zhang and Alleyne, 2005). To avoid this effect in active vehicle suspensions, Zhang and Alleyne proposed a reformulation of the problem such that the actuator tracks a desired trajectory rather than a desired force. Unfortunately, this method cannot be implemented on the loader because of the high relative degree between the measurable variables (chassis acceleration and boom position).

Active vibration damping of civil engineering structures often makes use of modal control, in which measured vibration is decomposed into separate modes and the control law is designed in uncoupled modal coordinates (Alkhatib and Golnaraghi, 2003). Such a system must consist of sufficient sensors and actuators to measure and control the desired modes. Although the skid-steer loader exhibits motion in multiple degrees of freedom, only a single actuator is available for vibration control.

As an alternative, the "skyhook damper" approach offers many of the benefits of state feedback with the simplicity of static output feedback (Karnopp, 1995). The idea is to define a control law such that the control input (force) is proportional to the velocity of the body with respect to a stationary inertial reference. In combination with position feedback, this scheme has been successfully implemented in many applications (see Camino, Zapieri and Peres, 1999, for example). Inertial "skyhook" damping is an appropriate choice for the skid-steer loader.

3.2 Control Design

The first step in designing a linear control law is converting the nonlinear model Eq. 25 to the familiar linear, time invariant (LTI) state space form (Eq. 38). This is essentially the same as Eq. 27, but with damping and actuator forces included and an expanded state vector for a set of first order differential equations.

$$\begin{aligned} \dot{\boldsymbol{x}} &= \mathbf{A}\boldsymbol{x} + \mathbf{B}u \\ \boldsymbol{y} &= \mathbf{C}\boldsymbol{x} \end{aligned} \tag{38}$$

$$\boldsymbol{x} = \begin{pmatrix} x_{\mathrm{H}} & \dot{x}_{\mathrm{H}} & y_{\mathrm{H}} & \dot{y}_{\mathrm{H}} & \theta_1 & \dot{\theta}_1 & \theta_2 & \dot{\theta}_2 \end{pmatrix}^{\mathrm{T}} \tag{39}$$

$$\boldsymbol{y} = \begin{pmatrix} \dot{x}_{\mathrm{H}} & \dot{y}_{\mathrm{H}} & \dot{\theta}_1 & \varphi \end{pmatrix}^{\mathrm{T}} \tag{40}$$

The system's single input u is the actuator force, F_{act}. The outputs are the chassis velocities and the boom angle φ. The pump and actuator dynamics are neglected for now, but will be revisited in a moment.

A static output feedback of the form $u = -\boldsymbol{K}_{\mathrm{fb}}\boldsymbol{y}$ acts as an inertial damper on the loader chassis for its three degrees of planar motion, plus a proportional position regulation to maintain the boom angle within a small range. The chassis velocities are difficult to measure directly, but can be easily approximated by integrating acceleration. The optimal gains $\boldsymbol{K}_{\mathrm{fb}}$ are determined by minimizing a linear quadratic cost function in terms of output feedback (Lewis, 1992). For the infinite horizon (steady state) case, the LQR objective function reduces to a function of the system's initial state or initial autocorrelation of the state (Eq. 41). The solution and feedback vector are obtained from the simultaneous solution of the three matrix equations Eq. 42.

$$J = \frac{1}{2}\int_0^\infty \left(\boldsymbol{x}^T\mathbf{Q}\boldsymbol{x} + uRu\right)dt \cong \frac{1}{2}\boldsymbol{x}^{\mathrm{T}}(0)\mathbf{P}\boldsymbol{x}(0) \tag{41}$$

$$\begin{aligned} &\mathbf{A}_{\mathrm{k}}^{\mathrm{T}}\mathbf{P} + \mathbf{P}\mathbf{A}_{\mathrm{k}} + \mathbf{C}^{\mathrm{T}}\boldsymbol{K}_{\mathrm{fb}}^{\mathrm{T}}R\boldsymbol{K}_{\mathrm{fb}}\mathbf{C} + \mathbf{Q} = \mathbf{0} \\ &\mathbf{A}_{\mathrm{k}}\mathbf{S} + \mathbf{S}\mathbf{A}_{\mathrm{k}}^{\mathrm{T}} + \boldsymbol{x}^{\mathrm{T}}(0)\boldsymbol{x}(0) = \mathbf{0} \\ &R\boldsymbol{K}_{\mathrm{fb}}\mathbf{C}\mathbf{S}\mathbf{C}^{\mathrm{T}} - \mathbf{B}^{\mathrm{T}}\mathbf{P}\mathbf{S}\mathbf{C}^{\mathrm{T}} = \mathbf{0} \end{aligned} \tag{42}$$

Although the boom lift cylinder is not in the ideal position and orientation for service as an active damper, it can still significantly attenuate the loader's disturbance response in the y and θ directions (see Fig. 12, for example).

Now that the structure of the active damping controller is clear, the question is how to produce the desired actuator damping force. The most direct way to accomplish this task would be to install a force sensor on one of the actuator joints and vary the pump flow rate to produce the desired force. To reduce the cost of implementation, the actuator piston-side pressure p_{A} is controlled instead. The rod side pressure p_{B} is connected to the charge line and its pressure does not vary as much. Friction increases the system damping, so neglecting its effect on actuator force serves the intended goal anyway.

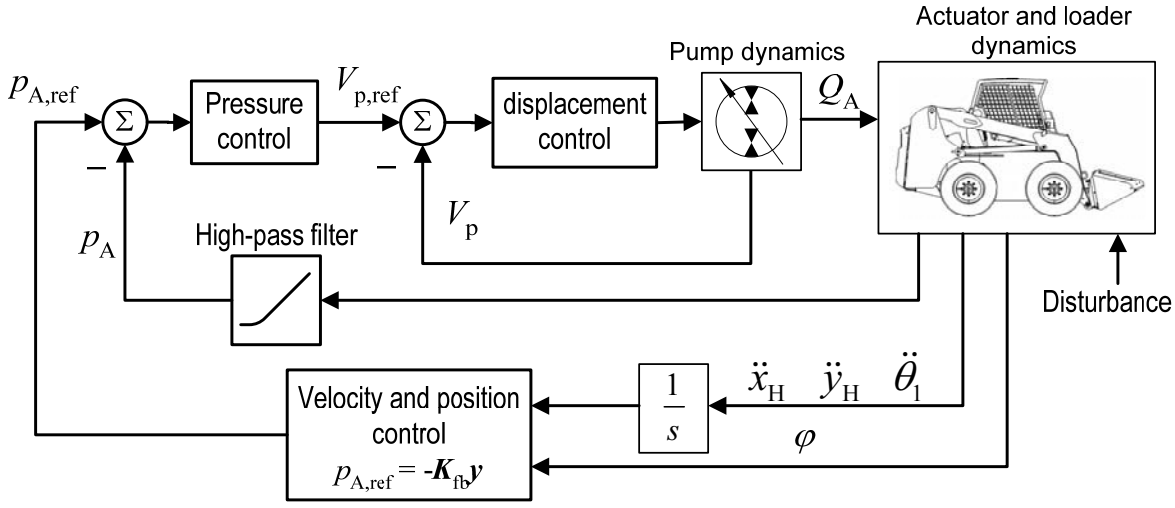

Fig. 11: *Control block diagram*

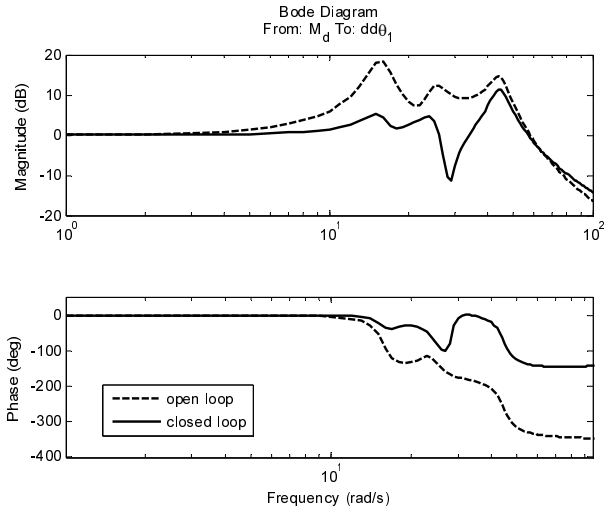

Fig. 12: *Effect of output feedback on frequency response of pitch disturbance transfer function*

The control structure consists of cascaded feedback loops, as shown in Fig. 11. The output feedback gives a reference pressure $p_{A,ref}$, which is tracked by a pressure control loop. The innermost loop controls the pump displacement V_p, which is nearly proportional to the outlet flow rate at constant rotational speed. A simple proportional pressure feedback $V_{p,ref} = k_p(p_{A,ref} - p_A)$ was found to provide acceptable performance with good robustness to the nonlinear rate limitation characteristic of the variable displacement pump, as discussed in section 2.4. The closed loop dynamics of the actuator pressure can be approximated by a reduced-order transfer function, Eq. 43.

$$\frac{p_A(s)}{p_{A,ref}(s)} = \frac{2810s - 6361}{s^3 + 222.3s^2 + 6328s + 78910} \tag{43}$$

For calculating gains, Eq. 43 was combined with Eq. 38 so that actuator dynamics were included in the loader model and the output LQR algorithm guaranteed stability.

3.3 Control Implementation

The active damping control law was implemented on the DC skid-steer loader with an 800 MHz embedded PC running Mathworks xPC Target real-time operating system. The sampling time was 1 ms. A few modifications to the controller were necessary for practical implementation. Pressure feedback required that the actuator pressure signal be passed through a high-pass filter to remove the steady state component due to the weight of the boom and bucket. Loader velocity was calculated from measured acceleration with a semi-integrator of the form $\frac{1}{s+\tau}$ with a small τ to avoid the signal drift associated with pure integration. The feedback gains $\boldsymbol{K}_{fb}$ were fine-tuned online. Parameter values are listed in Table 3. All feedback and control signals were normalized, so the gains are dimensionless. The infinity norm (maximum absolute value) for normalizing feedback signals was 19.62 m/s^2 (2 g) for linear acceleration, 20 rad/s^2 for angular acceleration and 33° for angular position. For the pressure feedback loop, $\|p_A\|_\infty$ was 100 bar with an empty loader bucket and 200 bar with a concrete-filled bucket.

Table 3: Control parameters

Parameter	Value	Unit
$\boldsymbol{K}_{fb}$	$(2.75 \;\; 5.10 \;\; -4.0 \;\; -0.22)$	-
τ	10	rad/s
k_p	0.5	-

Linear chassis acceleration was measured with a tri-axial accelerometer mounted on the side of the loader at its center of gravity (point H in Fig. 6). Pitch acceleration was estimated by measuring vertical acceleration with another sensor near the front of the chassis, calculating the difference between its value and $\ddot{y}_H$, and dividing by the distance between them.

The control law described in section 3.2 requires acceleration feedback, with pressure feedback in a cascaded loop. An even simpler method is based on pressure regulation only, i.e. $p_{A,ref} = 0$. Such an approach could be termed a "virtual accumulator" or passivity based controller because it operates according to the same principle as connecting an accumulator to the actuator. The virtual accumulator controller was also implemented and tested for comparison to active damping with acceleration feedback.

4 Vehicle Measurement

4.1 Parameter Identification

Most of the model parameters, such as geometry and mass properties, were obtained from the manufacturer. Parameters related to the tires and hydraulic seals had to be identified empirically.

4.1.1 Measurement of Actuator Friction

Measurements of actuator friction were conducted on the skid-steer loader. The boom cylinders were repeatedly extended and retracted with varying rates and loads. Since a direct force measurement was not available, friction was calculated from pressures and cylinder motion according to Eq. 44. In this equation, F_f is the friction force, F_L is the load force on the actuators due to the weight of the boom and bucket, and m_{eq} is the equivalent linear inertia of the boom and bucket. With known load masses, weight and inertia could be accurately estimated. Acceleration was calculated from measured position.

$$F_f = m_{eq}\ddot{x}_{act} + F_L - A_p\left(p_A - \alpha p_B\right) \tag{44}$$

Mixed friction is often modelled with the Stribeck curve, Eq. 45, with static, Coulomb, and viscous friction terms. Intuition suggests that seal friction should also be a function of fluid pressure.

$$F_f = f_s e^{-\tau_s|v|}\text{sign}(v) + f_C\text{sign}(v) + f_v v \tag{45}$$

The best fit to the friction data was obtained by modifying Eq. 45 so as to make the Coulomb friction dependent on both pressure and velocity and using a hyperbolic

tangent function as a continuous approximation of sign(v).

$$F_{\mathrm{f}} = f_{\mathrm{s}} e^{-\tau_{\mathrm{s}}|\dot{x}_{\mathrm{act}}|} \tanh(\gamma \dot{x}_{\mathrm{act}}) + f_{\mathrm{C}} p_{\mathrm{A}} + f_{\mathrm{v}} \dot{x}_{\mathrm{act}} \tag{46}$$

The linear coefficients in Eq. 46 were identified by multiple least-squares regression. The nonlinear coefficients (τ_{s} and γ) were also identified iteratively to minimize the sum of squared errors. Coefficient values are tabulated along with the R^2 and standard deviation s for the regression model in Table 4.

Table 4: Friction coefficients

Parameter	Value	Unit
f_{s}	17.0	kN
τ_{s}	40	s/m
γ	5.7	s/m
f_{C}	10.7	N/bar
f_{v}	8.13	kN·s/m
R^2	0.831	-
s	0.767	kN

4.1.2 Measurement of Fluid Compressibility

A similar test was conducted to identify parameters for seal leakage and fluid compressibility. The objective was to identify parameters in Eq. 36, where the volumetric leakage across the piston seals is a function of pressure and velocity (Eq. 47).

$$Q_{\mathrm{L}} = k_{\mathrm{Lp}} \left(p_{\mathrm{A}} - p_{\mathrm{B}} \right) - k_{\mathrm{Lv}} \dot{x}_{\mathrm{act}} \tag{47}$$

The boom cylinders were repeatedly extended and retracted while measuring boom angle, pump swash plate position, and pressure at the pump inlet and outlet ports. The actuator velocity was calculated kinematically from the boom velocity. Flow rate Q_{A} was estimated from pump displacement. Equation 36 was rearranged to be linear in the coefficients for least squares regression (Eq. 48). Parameter values are listed in Table 2 along with standard deviation estimate s.

$$\begin{aligned} Q_{\mathrm{A}} - \dot{x}_{\mathrm{act}} A_{\mathrm{p}} &= C + \frac{1}{K_{\mathrm{oil}}} \dot{p}_{\mathrm{A}} V_{\mathrm{A}} \\ &+ k_{\mathrm{Lp}} \left(p_{\mathrm{A}} - p_{\mathrm{B}} \right) + k_{\mathrm{Lv}} \dot{x}_{\mathrm{act}} \end{aligned} \tag{48}$$

Because derivatives of pressure and cylinder position were calculated numerically, signal noise presented more of a concern. A robust regression algorithm was used to reduce the influence of noise.

Table 5: Parameter values for fluid compressibility and actuator seal leakage

Parameter	Value	Unit
C	-3.2e-4	m^3/s
K_{oil}	1.64e9	Pa
k_{Lp}	2.87e-11	$m^3/s \cdot Pa$
k_{Lv}	-5.0e-4	m^2
s	2.09e-4	m^3/s

5.3 Measurement of Vehicle Vibration

Active damping performance was evaluated by measuring acceleration perceived by the vehicle operator while driving over obstacles on a test course. Vibration was measured and analyzed according to the basic evaluation method specified by ISO 2631-1 (1997). A specially designed accelerometer mounted on a rubber pad (PCB Piezotronics 356B41) was placed in between the operator and the seat. Translational acceleration at the seat's supporting surface was measured in three directions (a_{x}, a_{y}, a_{z}). Angular acceleration a_θ was estimated as described in section 3.3.

The raw acceleration signal in each direction i was weighted by a corresponding filter $W_{\mathrm{i}}(\mathrm{s})$ according to human sensitivity to vibration, giving the frequency weighted acceleration $\boldsymbol{a}_{\mathrm{wi}} = W_{\mathrm{i}}(\boldsymbol{a}_{\mathrm{i}})$. The root-mean-square value of each weighted acceleration signal was then calculated, as in Eq. 49. Total vibration exposure was then determined by combining the weighted RMS accelerations according to Eq. 50 where $k_{\mathrm{i}} = 1$ for the linear directions and $k_\theta = 0.4$.

$$a_{\mathrm{wi}} = \left[\frac{1}{T} \int_0^T \boldsymbol{a}_{\mathrm{wi}}^2 (t)\, dt \right]^{1/2} \tag{49}$$

$$a_{\mathrm{total}} = \left(k_{\mathrm{x}}^2 a_{\mathrm{wx}}^2 + k_{\mathrm{y}}^2 a_{\mathrm{wy}}^2 + k_{\mathrm{z}}^2 a_{\mathrm{wz}}^2 + k_\theta^2 a_{\mathrm{w}\theta}^2 \right)^{1/2} \tag{50}$$

Vehicle vibration was measured at low and high drive speeds (9 and 18 km/h) and low and high bucket masses (340 and 770 kg). The test course consisted of five wooden boards 4 cm tall spaced evenly on a paved concrete surface. The obstacle spacing was 6 m for low speed and 9 m for high speed. Four trials were repeated for each combination of speed, load and control. The four control conditions tested were (1) baseline condition with no extra damping, (2) passive damping with accumulators, (3) active damping by pressure regulation, "virtual accumulator", (4) active damping by multi-DOF velocity regulation, "skyhook damper". Figure 15 compares the mean a_{total} for each measured condition. Table 6 lists the mean change in total vibration and t-test p-values compared to the baseline for each combination of load and vehicle speed.

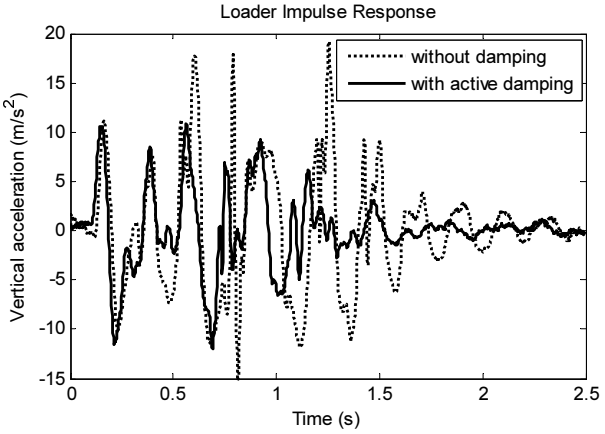

Fig. 13: *Vertical acceleration measured at seat while driving over a single obstacle at 9 km/h with empty bucket, with and without active "skyhook" damping*

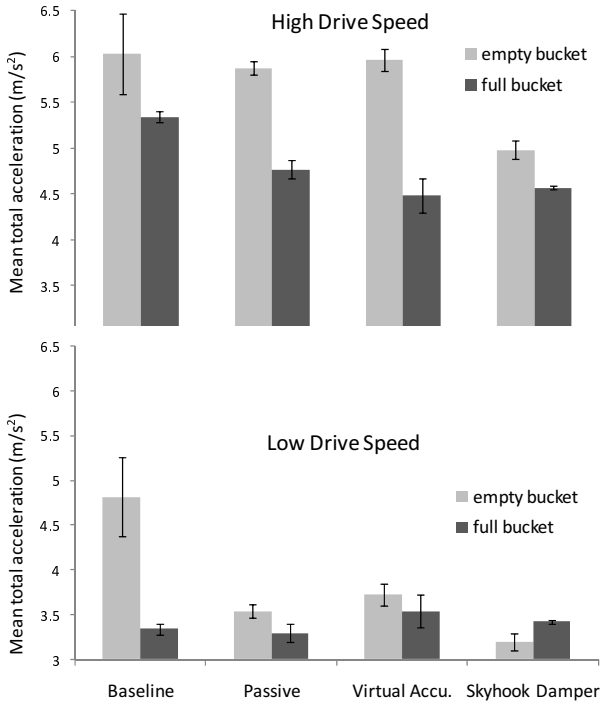

Fig. 14: *Vibration measurement summary. Error bars denote 95% confidence intervals*

Table 6: Reduction of total acceleration for passive and active damping methods

Speed/ Load	Stats	Passive Damping	Virtual Accu.	Skyhook Damper
Low	Δ (%)	-26.4	-22.6	-33.6
Low	p-value	0.0001	0.0003	0.0000
Low	Δ (%)	-1.3	6.0	2.5
High	p-value	0.2683	0.0159	0.0046
High	Δ (%)	-2.6	-1.1	-17.4
Low	p-value	0.1548	0.6377	0.0004
High	Δ (%)	-10.7	-16.1	-14.4
High	p-value	0.0038	0.0007	0.0008

Vehicle measurements clearly demonstrated the effectiveness of active vibration damping. Multi-DOF velocity feedback provided the best performance overall, reducing total acceleration up to 34 %. The combination of low travel speed and high bucket load produced relatively small accelerations; vehicle vibration was more or less the same with or without additional damping for that case. For all other trials, active damping with velocity feedback significantly improved ride comfort and outperformed the commercial passive accumulators. Results for the active virtual accumulator were about the same as the passive system.

5 Conclusions

The objective of this paper was to develop and demonstrate an active vibration damping system for a displacement controlled skid-steer loader using the boom lift cylinders as the control actuator. The main topics are summarized as follows:

A 4-DOF multibody vehicle model was developed to describe the motion of the loader chassis and boom.

Dynamic characteristics of the electro-hydraulic pump and boom lift actuators were modeled. Parameters related to the actuator seal leakage and friction were identified experimentally.

An active damping control law was designed based on static output feedback of the loader velocity for three directions of planar motion, plus the boom angle.

The control input for vibration damping is a force, so cascaded feedback loops of pump displacement and pressure were required to create the desired force. The pump's dynamic response has a strong effect on the active damping performance, particularly for large amplitudes.

Measurements indicated that the active damping system reduced total vibration by up to 3 4%, consistently surpassing passive dampers. An abbreviated algorithm utilizing only pressure and position measurements reduced vibration by ≤ 23 %.

Experimental results provide sufficient proof that the concept of active vibration damping without additional actuators can be applied successfully to a skid-steer loader. A more rigorous assessment of parameter variation and controller robustness will be presented in a future publication. The significance of angular motion in the roll direction (rotation about the *x*-axis) will also be considered in a future work.

Nomenclature

α	cylinder piston area ratio	[-]
φ	boom angle relative to chassis	[rad]
γ	actuator angle relative to horizontal	[rad]
θ_1	angular position of loader chassis relative to global coordinate frame	[rad]
θ_2	angular position of loader boom relative to global coordinate frame	[rad]
ω	frequency	[rad/s]
ζ	damping ratio	[-]
Δ	mean change in measured total vibration	[%]
A_p	cylinder piston area	[m²]
A_r	cylinder rod area	[m²]
F	force	[N]
F_{act}	hydraulic actuator force	[N]
F_f	actuator friction force	[N]
J	centroidal mass moment of inertia	[kg·m^2]
K_{oil}	fluid bulk modulus of elasticity	[Pa]
$\boldsymbol{K}_{fb}$	output feedback gain vector	[-]
M_d	disturbance moment	[N·m]
Q	flow rate	[m^3/s]
V	fluid volume	[m^3]
V_p	pump displacement volume	[m^3/rev]
c_t	coefficient of tire damping	[kg/s]
k_{eq}	actuator equivalent stiffness	[N/m]
k_{Li}	coefficient of internal leakage	[m^3/Pa·s]
k_p	pressure feedback gain	[-]
k_t	coefficient of tire stiffness	[N/m]
m	mass	[kg]
p	fluid pressure	[Pa]
r	distance between two points	[m]
$\boldsymbol{r}$	position vector	[m]
x	horizontal position	[m]

x_{act}	actuator piston position	[m]
x_H	horizontal position of loader chassis center of gravity relative to global coordinate frame	[m]
v	actuator velocity	[m/s]
y	vertical position	[m]
y_H	vertical position of loader chassis center of gravity relative to global coordinate frame	[m]

References

Alkhatib, R. and **Golnaraghi, M.F.** 2003. Active Structural Vibration Control: A Review. *Shock and Vibration Digest,* Vol. 35, No. 5, pp. 367-383.

Berger, A.D. and **Patel, K.B.** 1999. *Active Ride Control System for Off-Road Vehicles*. US Patent No. 5,897,287.

Camino, J., Zampieri, D. and **Peres, P.** 1999. Design of a Vehicular Suspension Controller by Static Output Feedback. *Proceedings of the American Control Conference*, San Diego, California, USA.

Eggers, B., Rahmfeld, R. and **Ivantysynova, M.** 2005. An Energetic Comparison Between Valveless and Valve-Controlled Active Vibration Damping for Off-Road Vehicles. *The Sixth JFPS International Symposium on Fluid Power*, Tsukuba, Japan, 2005.

Frediani, S., Gianoglio, R. and **Weber, J.** 2004. Electro Hydraulic Active Ride Control. *Proceedings of the Fourth International Fluid Power Conference (4.IFK),* Dresden, Germany, 2004.

Grabbel, J. and **Ivantysynova, M.** 2005. An Investigation of Swash Plate Control Concepts for Displacement Controlled Actuators. *International Journal of Fluid Power*, Vol. 6, No. 2, pp. 19-36.

Hansen, M.R., Andersen, T.O. and **Conrad, F.** 2002. Control of Oscillations in Hydraulically Driven Off-Highway Vehicles. *Bath Workshop on Power Transmission and Motion Control (PTMC 2002)*, pp. 81-94.

Hesse, H. 1995. Active Oscillation Damping for Off Road Vehicles. *4th Scandinavian International Conference on Fluid Power (SICFP'95),* pp. 1152-1172, Tampere, Finland.

Heybroek, K. 2008. *Saving Energy in Construction Machinery using Displacement Control Hydraulics*. PhD Thesis. Division of Fluid and Mechanical Engineering Systems, Department of Management and Engineering, Linkoping University, Linkoping, Sweden.

Hrovat, D. 1997. Survey of Advanced Suspension Developments and Related Optimal Control Applications. *Automatica*, Vol. 33, No. 10, pp. 1781-1817.

International Organization for Standardization 1997. *ISO 2631-1 (1997): Mechanical vibration and shock - Evaluation of human exposure to whole-body vibration - Part 1: General Requirements.* International Organization for Standardization. Geneva, Switzerland.

Karnopp, D. 1995. Active and Semi-Active Vibration Isolation. *Journal of Mechanical Design*, Vol. 117, Issue B, pp. 177-186.

Klooster, S. 2004. *Vibration Suppression and Safety Seat Motion Design of a Hyper-Active Seat.* MS Thesis. School of Mechanical Engineering, Georgia Institute of Technology, USA, pp. 113-119.

Latour, C. and **Biener, R**. 2002. Comparison of Active and Passive Oscillation Suppression Systems for Wheel Loaders. *3.IFK (3rd Int. Fluid Power Conference)*, T4 Vol. 2, S. 101-112, Aachen, Germany.

Lewis, F. 1992. *Applied optimal control and estimation*. Prentice-Hall, Inc. Englewood Cliffs, New Jersey, USA, pp. 191-200.

Nikravesh, P. 2008. *Planar multibody dynamics: formulation, programming, and applications*. CRC Press. Boca Raton, Florida, USA.

Rahmfeld, R. and **Ivantysynova, M.** 2004. An Overview about Active Oscillation Damping of Mobile Machine Structure. *International Journal of Fluid Power*, Vol. 5, No. 2, pp. 5-24.

Rahmfeld, R. and **Ivantysynova, M.** 2003. New Displacement Controlled Linear Actuator Technology – A Suitable Control Element for Active Oscillation Damping. *The Eighth Scandinavian International Conference on Fluid Power, SICFP'03,* May 7-9, 2003, Tampere, Finland.

Rahmfeld, R., Ivantysynova, M. and **Eggers, B.** 2004. Active Vibration Damping for Off-Road Vehicles Using Valveless Linear Actuators. *Proceedings of the SAE Commercial Vehicle Engineering Congress & Exhibition*, Chicago, IL, USA. SAE Technical Paper 2004-01-2655.

Williamson, C. 2007. *Active Vibration Damping for a Skid Steer Loader Using Displacement Controlled Actuators*. MS Thesis. School of Mechanical Engineering, Purdue University, West Lafayette, Indiana, USA.

Williamson, C. and **Ivantysynova, M.** 2007. The Effect of Pump Efficiency on Displacement-Controlled Actuator Systems. *Proceedings of the Tenth Scandinavian International Conference on Fluid Power (SICFP '07),* Tampere, Finland, Vol. 2, pp. 301-326.

Zhang, Y. and **Alleyne, A.** 2005. A practical and effective approach to active suspension control. Vehicle System Dynamics, Vol. 43, No. 5, pp. 305-330.

Zuo, L. and **Nayfeh, S.A**. 2003. Low order continuous-time filters for approximation of the ISO 2631-1 human vibration sensitivity weightings. *Journal of Sound and Vibration*, 265, pp. 459-465.

Christopher Williamson
Mr. Williamson is from the USA. He received his BS degree from Brigham Young University in 2005 and MS from Purdue University in 2007, both in Mechanical Engineering. He is currently a PhD student at Purdue University in the Dept. of Agricultural & Biological Engineering. His main research topic is energy-efficient fluid power control systems.

Monika Ivantysynova
Born on December 11th 1955 in Polenz (Germany). She received her MSc. Degree in Mechanical Engineering and her PhD. Degree in Fluid Power from the Slovak Technical University of Bratislava, Czechoslovakia. After 7 years in fluid power industry she returned to university. In April 1996 she received a Professorship in fluid power & control at the University of Duisburg (Germany). From 1999 until August 2004 she was Professor of Mechatronic Systems at the Technical University of Hamburg-Harburg. Since August 2004 she is Professor at Purdue University, USA. Her main research areas are energy saving actuator technology and model based optimisation of displacement machines as well as modelling, simulation and testing of fluid power systems. Besides the book "Hydrostatic Pumps and Motors" published in German and English, she has published more than 80 papers in technical journals and at international conferences.

Shinok Lee
Shinok received his B.S. degree from Purdue University in 2008 in Mechanical Engineering. He is continuing his studies as a Master's student at Purdue University in the Dept. of Mechanical Engineering. His main research topic is active vibration control of mobile hydraulic machines. He originally comes from Seoul, South Korea and is currently working with a great team at Maha Fluid Power Research Center.